Bitlis Eren Üniversitesi Fen Bilimleri Dergisi
BİTLİS EREN UNIVERSITY JOURNAL OF SCIENCE
ISSN: 2147-3129/e-ISSN: 2147-3188
VOLUME: 12 NO: 3 PAGE: 764-772 YEAR: 2023
DOI:10.17798/bitlisfen.1297654

Preparation of Transparent ZIF-8/TiO_2 Nanocomposite Thin Films for Photocatalytic Applications

Onur İLOĞLU[1], Hüsnü Arda YURTSEVER[1*]

[1]*Adana Alparslan Türkeş Science and Technology University, Faculty of Engineering, Department of Materials Science and Engineering, Adana, Türkiye*
(ORCID: 0000-0003-3410-1072), (ORCID: 0000-0002-1920-8149)

Keywords: Photocatalysis, Thin film, Nanocomposite, ZIF-8, TiO_2.

Abstract
Transparent ZIF-8/TiO_2 nanocomposite thin films were prepared by a two-stage dip-coating method. TiO_2 was first deposited on glass substrates by sol-gel dip-coating. Heat treatment temperature, number of layers, and doping metal type or level were optimized in the first step. In the next step, ZIF-8 was grown by solvent-based crystallization method on TiO_2 layers. Cu, Ce, Fe, or Zn-doped TiO_2 thin films were prepared in order to increase the photocatalytic performance of the ZIF-8/TiO_2 nanocomposite. The highest photocatalytic methylene blue degradation activities were obtained with the ZIF-8/TiO_2 nanocomposite thin films prepared by using 1% Cu or 1% Ce-doped TiO_2 thin films as the substrates. Both films exhibited 19% dye removal in 1 hour under 254 nm LED light irradiation, whereas the dye removal efficiencies were 36% and 29% , respectively, in 1 hour under 365 nm LED light irradiation.

1. Introduction

Scientific studies report that by 2050, energy and clean water demand will increase by 80% and 55%, respectively, due to an increase in the world population to 9.7 billion people [1]. Using clean and renewable energy sources and implementing new water treatment technologies with low energy requirements and high efficiencies are of great importance in ensuring a sustainable environment. Photocatalysis stands out as a promising method for the generation of clean hydrogen from water and the oxidation of water pollutants by the utilization of solar energy, which is abundant and free. Photocatalyst design and preparation, which are at the center of photocatalysis, are the most important steps that determine the efficiency of any photocatalytic process. Metal-organic frameworks (MOFs), which have been frequently used in photocatalysis in recent years, are promising materials due to their microporous structure and high surface area. ZIF-8 (Zeolitic imidazolate framework-8), which consists of zinc and 2-methyl imidazole building blocks and is in the zeolitic imidazolate family, has a high surface area (1500-2500 m^2/g), high thermal stability, and an appropriate surface structure for the adsorption of organic pollutant molecules in water [2]. ZIF-8 also has chemical resistance to aqueous alkaline solutions and organic solvents [3].

ZIF-8 is a semiconductor material with a high band gap energy (5.2 eV) and was used in the form of a nanocomposite with zinc, copper, iron, cadmium, bismuth, or carbon-based materials to improve its photocatalytic properties [4] in pollutant oxidation, heavy metal, and CO_2 reduction, NO removal, conversion of nitrogen to ammonia, or adsorption [5]-[16]. It was revealed that these nanocomposite structures showed higher photocatalytic activities in the specified applications compared to their pure form. ZIF-8 was also doped to improve its photocatalytic activity [17], [18]. Studies have shown that when ZIF-8 is used in combination with different semiconductor materials, the light absorption edge can be reduced to the visible light region. The reason for the higher activities obtained with doped or nanocomposite ZIF-8 compared to undoped or non-

*Corresponding author: husnuarda@gmail.com
Received: 16.05.2023, Accepted: 18..09.2023

composite structures was reported to be the faster transport and separation of electron-hole pairs due to heterojunctions formed on the photocatalyst surface. Studies have shown that photocatalytic activity does not only depend on light absorption properties but also on the presence of heterojunctions or structural defects in the structure [13], [19].

TiO_2 is a widely used photocatalyst due to its high activity and high chemical and photochemical stability [20]. ZIF-8 was prepared together with TiO_2 in nanocomposite form for the degradation of organic pollutants or for reduction reactions [19], [21]-[25]. The effects of the use of ZIF-8 together with TiO_2 in nanocomposite form were mostly investigated in powder form. A limited number of studies on ZIF-8 films were conducted in which different substrates were used, such as ITO/FTO [26], [27], functionalized glass [28], Au [29], [30], copper [31], or Si [32] surfaces. Those studies were on the synthesis and characterization of ZIF-8 films, and the activities of the prepared films in photocatalysis were not investigated. The use of photocatalyst films is more convenient due to the ease of application, which mostly doesn't require a photocatalyst recovery step, and the use of fewer amounts of valuable photocatalytic material compared to bulk powder form.

The aim of this study was to prepare ZIF-8/TiO_2 nanocomposite thin films and to increase the photocatalytic activity of bare ZIF-8, which is quite low compared to TiO_2. An optimization was conducted by varying parameters such as heat treatment temperature, number of layers, and amount and type of metal doping in order to find the appropriate TiO_2 support on which ZIF-8 crystals would be grown.

2. Materials and Method

2.1. Thin Film Preparation

The first step in the preparation of transparent ZIF-8/TiO_2 thin films was the optimization of the TiO_2 layer on which ZIF-8 crystallites would be grown. In these studies, the heat treatment temperature, number of TiO_2 layers, dopant metal type, and concentration were optimized by considering the photocatalytic activities. Undoped and doped TiO_2 sols were prepared with titanium:water:acid molar ratios of 1:2:0.057. Titanium tetraisopropoxide (TTIP, Aldrich 97%) was used as the titanium precursor; copper nitrate trihydrate (99.5%, Merck), cerium nitrate hexahydrate (99.5%, Alfa Aesar), iron nitrate nonahydrate (99%, Merck), and zinc nitrate hexahydrate (98%, Aldrich) were used as the dopant precursors; ethanol (absolute Aldrich), nitric acid (HNO_3, 65%, Merck) and ultra-pure water were used as solvents. Undoped TiO_2 sols were prepared by the dropwise addition of an ethanolic solution of water and nitric acid (0.555 mL H_2O, 0.065 mL HNO_3 and 50 mL ethanol) to an ethanolic solution of TTIP (5 mL TTIP and 50 mL ethanol). Metal-doped TiO_2 sols were prepared by the same procedure and recipe in which the ethanolic solution of water and nitric acid contained predetermined amounts of metal precursors. Due to the aqueous nature of the metal salts, the water originating from these salts was subtracted from the water in the main recipe to ensure a titanium:water molar ratio of 2. The sols were aged at room temperature for 15 minutes before coating.

TiO_2 thin films were coated on a 7.5x2.5 cm borosilicate glass substrate by using the dip-coating technique. A clean surface is of great importance for homogeneous and continuous glass surface coating. For this reason, the glass substrates were first soaked in detergent water, then soaked in water, acetone, and ethanol in an ultrasonic bath, then washed with ethanol and dried with nitrogen. Cleaned substrates were then coated with TiO_2 by the dip-coating method. Substrate removal rates were optimized before the preparation of TiO_2 and ZIF-8/TiO_2 nanocomposite thin films. The dipping rate was set to 200 mm/min. A removal rate of 200 mm/min, which was determined in the optimization studies, was used in the preparation of TiO_2 and ZIF-8/TiO_2 thin films.

In the first step, undoped TiO_2 thin films were prepared, dried at room temperature, and then heat treated at 400, 450, 500, and 550^{o}C for 3 hours. In the next step, metal-doped TiO_2 thin films were prepared and heat-treated at 400^{o}C. Cerium, iron, copper, and zinc-doped TiO_2 thin films with doping amounts ranging from 1-10 mol% were then prepared, and ZIF-8 was coated on these TiO_2 thin films. Zinc nitrate and 2-methylimidazole (Hmim, 99%, Aldrich) were used for the formation of ZIF-8 crystals on TiO_2 surfaces. The final molar ratios of Zn^{2+}:Hmim:methanol were set to 1:8:700, which is typical for ZIF-8 synthesis [17]. Zinc nitrate and 2-methylimidazole were stirred in 45 mL of methanol in separate beakers (50 mL) at room temperature. These solutions were added simultaneously to a beaker (100 mL) in which TiO_2 thin film-coated glass substrates were vertically immersed, and the final solution was stirred for 30 minutes at room temperature. The immersion time was optimized based on preliminary experiments. The transparency and homogeneity of the film grown for 30 minutes were better compared to the films grown for 15, 45, and 60 minutes, whereas the photocatalytic activities were similar. The coated films were washed

consecutively with methanol and ethanol and dried at 80°C for 24 hours. For comparison, bare ZIF-8 film on a glass substrate was also synthesized. The glass substrate was first functionalized by silanization. The cleaned glass substrate was kept immersed in a 2% (by volume) methanolic solution of trimethoxymethylsilane (Aldrich, 98%) for 4 hours. The glass substrate was then washed consecutively with methanol and ethanol and dried before coating. The procedure and recipe used in growing ZIF-8 crystals on TiO_2 thin films were used for the preparation of bare ZIF-8 film on a glass substrate.

2.2. Characterization

The optical characterization of the prepared films was carried out by an Agilent Cary60 UV-Vis Spectrophotometer. The light transmittances of the films were recorded in the 300-800 nm wavelength range. Surface morphology and film thickness were investigated by Scanning Electron Microscopy (SEM) with the FEI Quanta 650 Field Emission. Thickness and average grain size were calculated by using SEM images.

2.3. Photocatalytic Tests

The photoreaction system was constructed as shown in Figure 1. An 11 cm high and 10.5 cm wide Plexiglas box was used, and a glass container with a diameter of 4.8 cm and a height of 2.4 cm was placed at the bottom. A LED lamp with its maximum emission at 254 nm or 365 nm was placed on top of the box. Glass slides were cut so that the active surface area of a thin film was 2.5x2.0 cm^2. The films were placed horizontally (perpendicular to the light from the LED lamp) at the bottom of the glass container. Methylene blue solution (2 ppm, 5 mL) was used as the model dye solution. The samples withdrawn after 1-hour irradiation were analyzed by a UV-Vis spectrometer (Agilent, Cary60 UV-VIS Spectrophotometer). Dye removal (%) was calculated according to the following equation:

$$\text{Dye removal (\%)} = ((I_o - I) / I_o) * 100 \quad (1)$$

where I is the absorbance of the methylene blue solution sample and I_o is the absorbance of 2 ppm methylene blue solution. The absorbance value at the maximum absorption wavelength (664 nm) was used in the calculations. The performances of the films were also investigated under 365 nm light in order to show the interaction of ZIF-8 and TiO_2 with regard to the light absorption characteristics. The same setup was used. The only differences in these experiments were that 25 mL of methylene blue solution was used and that the solution was agitated continuously during the experiments. Photocatalytic activity determination experiments were carried out in duplicate runs.

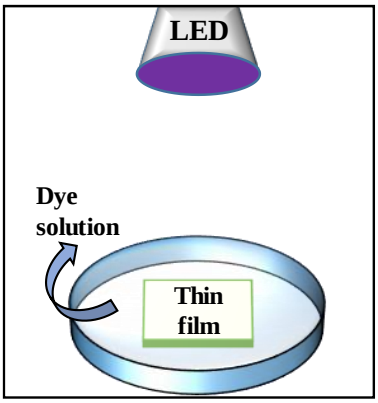

Figure 1. A schematic representation of the photocatalytic reaction setup.

3. Results and Discussion

3.1. Characterization

3.1.1. Optimization of Dip-coating Process

Dip-coating was carried out using removal rates in the range of 20-400 mm/min. Since the films will become thinner as the removal rate decreases, lower rates were also tried, but a wavy structure through the films was observed. At rates of 200 mm/min and above, it was found that this wavy structure did not exist and films of sufficient thinness were formed (no lifting from the surface or visible cracks were observed after heat treatment). Therefore, a removal rate of 200 mm/min was used in the subsequent studies. The photographs of the prepared TiO_2 thin films are shown in Figure 2.

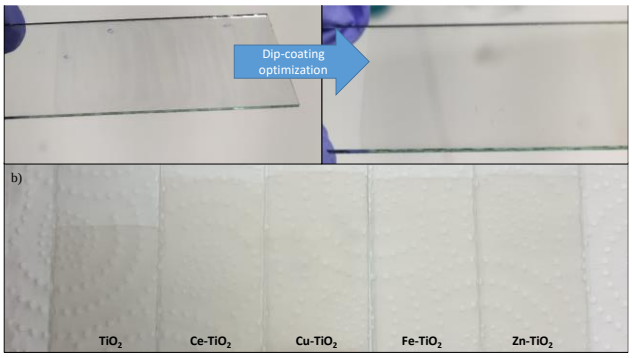

Figure 2. a) The photographs of TiO_2 thin films prepared in the optimization studies, b) Photographs of as-deposited undoped/doped TiO_2 thin films on glass substrates.

3.1.2. Morphologies of TiO_2 and ZIF-8/TiO_2 Nanocomposite Thin Films

The surface and cross-section morphology of the thin films were investigated by SEM analysis. SEM images of ZIF-8 uncoated and coated 1% Cu-doped TiO_2 and 1% Fe-doped TiO_2 thin films heat treated at 400°C are given in Figures 3 and 4, respectively. SEM images (Figures 3a and 4a) showed that ZIF-8 uncoated Cu and Fe doped TiO_2 thin films were homogeneously deposited on glass substrates. The average grain sizes of these films were determined to be 23 nm and 29 nm for 1% Cu-doped TiO_2 and 1% Fe-doped TiO_2, respectively.

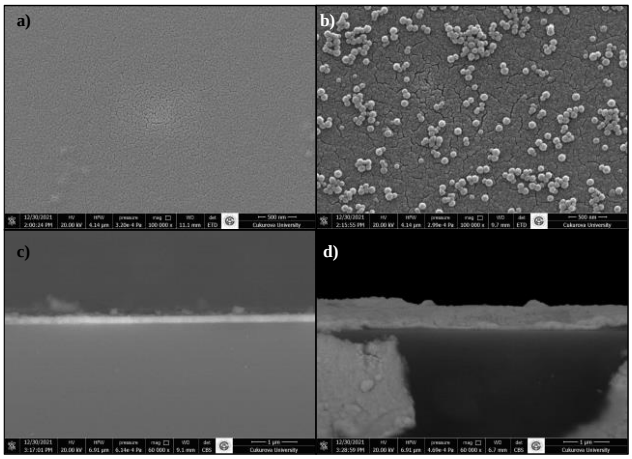

Figure 3. Surface and cross-section SEM images of 1% Cu doped TiO_2 thin films (a, c) and ZIF-8 / 1% Cu doped TiO_2 thin films (b, d).

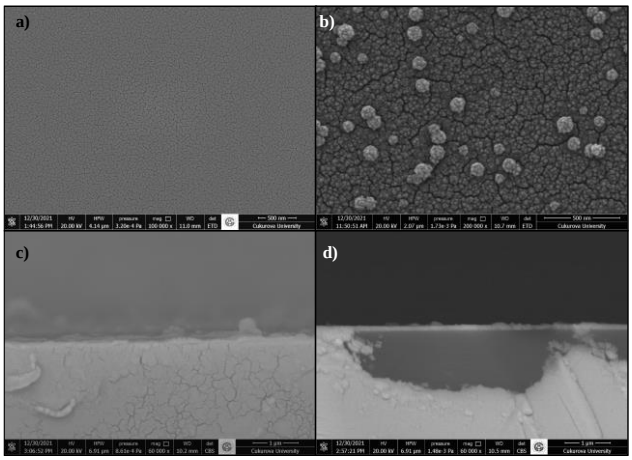

Figure 4. Surface and cross-section SEM images of 1% Fe doped TiO_2 thin films (a, c) and ZIF-8 / 1% Fe doped TiO_2 thin films (b, d).

It was observed that ZIF-8 particles grown on doped TiO_2 thin films were not homogeneously distributed on the surface (Figures 3b and 4b). ZIF-8 particles have spherical shapes, and the average grain sizes of the ZIF-8-coated thin films were determined to be in the 90-100 nm range. There were no significant differences between the average thicknesses of the uncoated and ZIF-coated thin films due to the inhomogeneity of ZIF-8 films. The average thicknesses were found to be in the 0.15-0.17 µm range.

3.1.3. Light Absorption Properties of TiO_2 and ZIF-8/TiO_2 Nanocomposite Thin Films

The light absorption properties of undoped and doped TiO_2 thin films, bare ZIF-8, and ZIF-8-coated TiO_2 thin films were determined by evaluating their UV-Vis transmittance spectra between 300 and 800 nm wavelength. The light transmission curves of these films are given in Figure 5. As seen in Figure 5a, the transmittance curve of undoped TiO_2 thin film heat treated at 400°C shifted to lower wavelengths when higher heat treatment temperatures were applied. This showed that the film heat-treated at 400°C has a higher light absorption capacity compared to the other films. The transmittance curves of Ce-doped TiO_2 thin films heat-treated at 400°C are shown in Figure 5b.

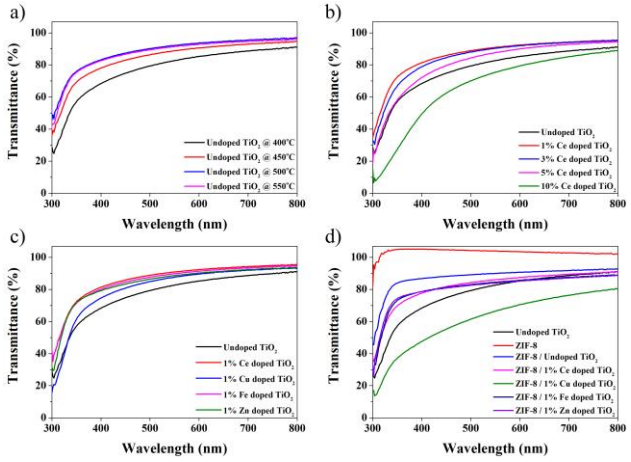

Figure 5. UV-Vis transmittance spectra of a) Undoped TiO_2 thin films heat treated at different temperatures, b) Ce Doped TiO_2 thin films heat treated at 400 °C, c) various metals doped TiO_2 thin films heat treated at 400 °C and d) ZIF-8, ZIF-8 coated various metals doped TiO_2 thin films heat treated at 400 °C.

It was observed that the transmittance curve of TiO_2 shifted to lower wavelengths at low doping levels (1, 3, 5%) and to higher wavelengths at high doping levels (10%). This finding showed that the light absorption of TiO_2 increased when doped with Ce at high doping levels. The transmittance curves of TiO_2 doped with different metals are shown in Figure 5c. It can be stated that the curve mainly shifted to

lower wavelengths when TiO_2 was doped with Ce, Cu, Fe, or Zn at a 1% doping level. Among the doped TiO_2 thin films, Cu-doped TiO_2 showed higher light absorption capacity compared to Ce, Fe, or Zn doped TiO_2 since the absorption edge of this film is at a higher wavelength. The transmittance curves of bare ZIF-8 and ZIF-8-coated TiO_2 thin films doped with different metals are shown in Figure 5d. ZIF-8-coated Cu-doped TiO_2 thin films showed higher light absorption capacities than the other ZIF-8-coated TiO_2 thin films and bare ZIF-8. The higher light absorption capacity of Cu-doped TiO_2 thin films may lead to higher photocatalytic activity than the other films. These findings indicated that the light absorption capacity and, as a result, the photocatalytic activity of bare ZIF-8 film may be increased when undoped or doped TiO_2 thin films are used as supports to grow ZIF-8 crystals.

3.2. Photocatalytic Performances of TiO_2 and ZIF-8/TiO_2 Nanocomposite Thin Films

Figure 6a shows how well dyes are removed by adsorption and photocatalysis from thin films of undoped TiO2 that have been heated at different temperatures. Photocatalytic removal efficiencies were higher than adsorptive removal efficiencies. This is an indication that photocatalytic degradation was achieved with the prepared films. The highest removal efficiencies by adsorption and photocatalysis were obtained with the film heat-treated at 400°C. With this film, 37% and 56% of the dye were removed by adsorption and photocatalysis, respectively. The film heat-treated at 400°C showed better photocatalytic performance than the films heat treated at 450, 500, and 550°C under 254 nm irradiation. Therefore, 400°C was chosen as the heat treatment temperature for further studies. After determining the optimum heat treatment temperature, the effect of the number of TiO_2 layers on the photocatalytic activity was investigated. Undoped TiO_2 thin films containing 1-4 layers were prepared, and their photocatalytic performances were evaluated. Figure 6b shows how well different numbers of layers of undoped TiO2 thin films treated at 400°C remove dye through photocatalysis. The photocatalytic performances are slightly different, as can be seen from Figure 6b. The photocatalytic dye removal efficiencies of monolayer and multilayer undoped TiO_2 thin films varied between 50 and 61%. In light of these results, it was decided to use monolayer TiO_2 thin films as a basis for the preparation of ZIF-8/TiO_2 nanocomposite thin films due to their ease of preparation.

TiO_2 thin films doped with Ce in the range of 1-10 mol% were prepared, and their photocatalytic performances were determined, in order to investigate the effect of doping level on the photocatalytic dye removal efficiency of TiO_2 and to find a suitable TiO_2 support on which ZIF-8 crystals will be grown.

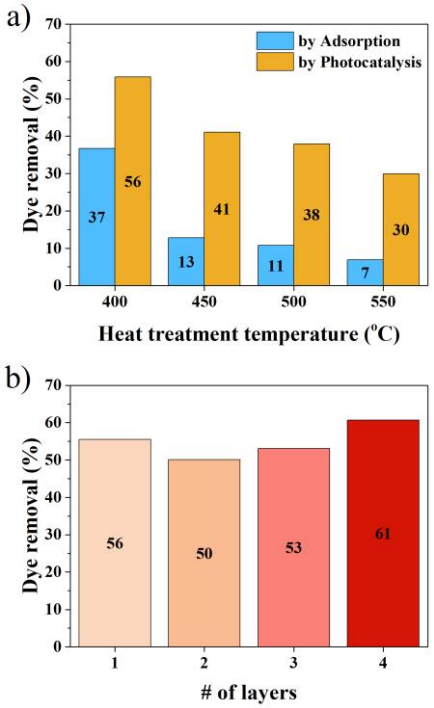

Figure 6. a) Dye removal efficiencies by adsorption and photocatalysis with undoped TiO_2 thin films heat treated at different temperatures, b) Photocatalytic dye removal efficiencies of undoped TiO_2 thin films heat treated at 400°C with different number of layers.

Before starting the photocatalytic performance determination experiments, a direct photolysis experiment was first performed to determine the contribution of spontaneous degradation of methylene blue under 254 nm light. The experiment was carried out in the absence of a photocatalyst film. It was found that 5% of the dye spontaneously self-degraded in 1 hour under 254 nm light. The photocatalytic dye removal efficiencies of Ce-doped TiO_2 thin films and dye removal by direct photolysis are given in Figure 7a. The highest activity was obtained with 1% Ce-doped TiO_2 thin films and a decrease in the photocatalytic activity was observed as the doping level increased. The photocatalytic dye removal efficiencies of TiO_2 thin films doped with various metals are given in Figure 7b. The highest activities were obtained with Ce and Fe-doped TiO_2 thin films. Zn doping had no significant effect on the photocatalytic activity, while Cu doping decreased the activity of TiO_2 under these conditions. Interaction with light is one of the parameters affecting photocatalytic activity. It is thought that photocatalytic activity will increase with an increase

in light absorption capacity. However, other parameters- such as the interaction of dye molecules with the surface and the separation efficiency of electron-hole pairs, also have significant effects on the activity. As can be seen in Figure 5, a red shift is observed in the metal-doped films only at the 10% doping level. However, when the photocatalytic activity results were analyzed (Figure 7), it was found that 1% of metal-doped films showed higher photocatalytic activity. Therefore, it can be interpreted that electron-hole pair separation and the interaction of dye molecules with the surface may be more efficient in 1% metal doped films compared to other films.

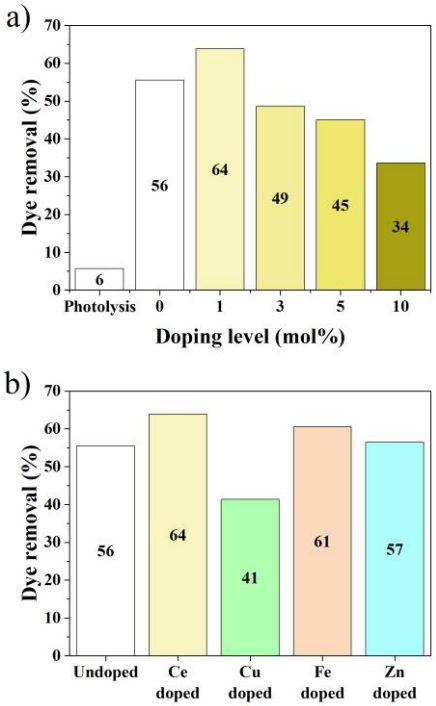

Figure 7. Photocatalytic dye removal efficiencies of a) Ce doped TiO_2 thin films and b) 1% various metals doped TiO_2 thin films.

In the final part, ZIF-8 was grown on 1% TiO2 thin films doped with various metals, and their photocatalytic performances were evaluated under both 254 nm and 365 nm LED light irradiation. The results are given in Figures 8a and 8b, respectively. The photocatalytic dye removal efficiencies of bare ZIF-8 film on glass substrate under both 254 nm and 365 nm LED irradiation are also given in Figure 8 for comparison.

The photocatalytic activity decreased when ZIF-8 was coated on TiO_2 films, according to Figures 7 and 8. The reason may be that ZIF-8 has a higher band gap energy than TiO_2, and the TiO_2 surface was blocked by ZIF-8 crystals, which prevented the interaction of TiO_2 with light. However, it should be noted that the activity of ZIF-8 increased when ZIF-8 was coated on TiO_2 films, which was the main aim of this study. According to Figure 8, ZIF-8/TiO_2 nanocomposite thin films obtained with 1% Ce and 1% Cu doped TiO_2 thin films showed higher activity in the photocatalytic removal of the dye under both 254 nm and 365 nm LED irradiation when compared to 1% Fe and 1% Zn doped TiO_2 thin films. In general, ZIF-8 grown on TiO_2 thin films showed better photocatalytic dye removal efficiencies compared to bare ZIF-8 grown on the glass substrate.

The highest photocatalytic activity was obtained with the ZIF-8 coated-, 1% Cu-doped TiO_2 film, which may be due to the formation of more efficient ZIF-8/TiO_2 heterojunctions and better light interaction. As seen in Figure 5d, a slue shift was observed in ZIF-8 coated films compared to the uncoated film, and among the ZIF-8 coated films, ZIF-8 coated Cu-doped TiO_2 thin film showed higher light absorption capacity compared to other films.

These results indicated that the photocatalytic activity of ZIF-8 could be improved when metal-doped TiO_2 substrates were used as supports for the growth of ZIF-8 crystals. According to these results, the photocatalytic activity of ZIF-8 can be enhanced by using TiO_2 thin film supports doped with low amounts of Ce, Cu, Fe, or Zn and heat treated at relatively low temperatures (400^{o}C).

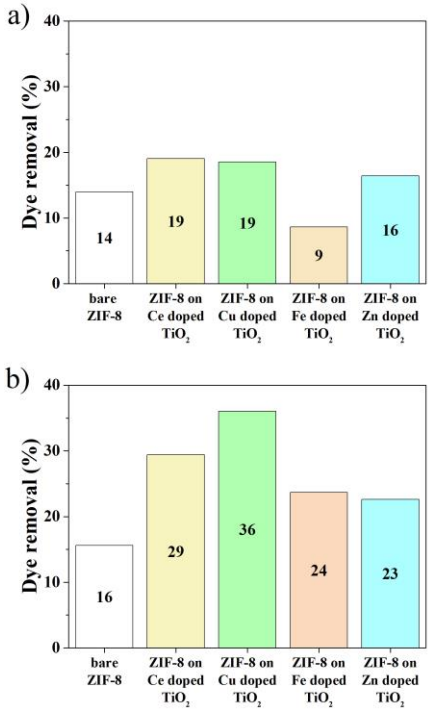

Figure 8. Photocatalytic dye removal efficiencies of bare ZIF-8 and ZIF-8/TiO_2 nanocomposite thin films: a) under 254 nm LED irradiation and b) 365 nm LED irradiation.

4. Conclusion and Suggestions

In this study, the optimization of TiO_2 support properties for the preparation of transparent ZIF-8/TiO_2 nanocomposite thin films was performed by evaluating their photocatalytic performances. According to the results, it was found that the photocatalytic dye removal efficiencies of ZIF-8/TiO_2 nanocomposite thin films prepared by 30-min ZIF-8 growth on 1% Ce, Cu, Fe, and Zn doped TiO_2 thin films heat treated at 400^{o}C were higher than those of bare ZIF-8 thin films grown on glass substrates. The highest photocatalytic dye removal efficiencies were obtained with ZIF-8/TiO_2 nanocomposite thin films prepared with 1% Ce and 1% Cu-doped TiO_2 thin films. The order of magnitude of the photocatalytic dye removal efficiencies did not change with the change of irradiation source (254 nm or 365 nm LED lamps) used in this study. The ZIF-8-coated 1% Cu and 1% Ce-doped TiO_2 films removed 19% of the dye under a 254 nm LED light in 1 hour. Their dye removal efficiencies under 365 nm LED light increased to 36% and 29%, respectively. All ZIF-8/TiO_2 nanocomposite thin films showed higher activities than the bare ZIF-8 film, indicating that the activity of ZIF-8 can be enhanced when grown on TiO_2 surfaces doped with 1% Ce, Cu, Fe, or Zn metals. These findings indicate that a nanocomposite structure containing ZIF-8 and TiO_2 can be prepared as transparent thin films, and the photocatalytic activity of ZIF-8 can be improved by the optimization of TiO_2 support.

Acknowledgment

This study was supported by Adana Alparslan Türkeş Science and Technology University Scientific Research Coordination Unit, Türkiye. Project Number: 20303001. Onur İloğlu was supported by the TÜBİTAK-BİDEB 2210-C National Scholarship in Priority Fields in Science Program for MSc students.

Contributions of the authors

Onur İloğlu: literature review, investigation, evaluation of data, writing/reviewing/editing.

Hüsnü Arda Yurtsever: conceptualization, literature review, evaluation of data, writing/reviewing/editing.

Conflict of Interest Statement

There is no conflict of interest between the authors.

Statement of Research and Publication Ethics

The study is complied with research and publication ethics.

References

[1] B. L. Loeb, "Water-Energy-Food Nexus," *Ozone: Science & Engineering,* vol. 38, no. 3, pp. 173-174, 2016, doi: 10.1080/01919512.2016.1166029.

[2] H. Dai *et al.*, "Recent advances on ZIF-8 composites for adsorption and photocatalytic wastewater pollutant removal: Fabrication, applications and perspective," *Coordination Chemistry Reviews,* vol. 441, p. 213985, 2021, doi: 10.1016/j.ccr.2021.213985.

[3] K. S. Park *et al.*, "Exceptional chemical and thermal stability of zeolitic imidazolate frameworks," *PNAS,* vol. 103, no. 27, pp. 10186-10191, Jul 5 2006, doi: 10.1073/pnas.0602439103.

[4] H.-P. Jing, C.-C. Wang, Y.-W. Zhang, P. Wang, and R. Li, "Photocatalytic degradation of methylene blue in ZIF-8," *RSC Advances,* vol. 4, no. 97, pp. 54454-54462, 2014, doi: 10.1039/c4ra08820d.

[5] A. Chakraborty, D. A. Islam, and H. Acharya, "Facile synthesis of CuO nanoparticles deposited zeolitic imidazolate frameworks (ZIF-8) for efficient photocatalytic dye degradation," *Journal of Solid State Chemistry,* vol. 269, pp. 566-574, 2019, doi: 10.1016/j.jssc.2018.10.036.

[6] A. Liu *et al.*, "Construction of $CuInS_2$@ZIF-8 nanocomposites with enhanced photocatalytic activity and durability," *Materials Research Bulletin,* vol. 112, pp. 147-153, 2019, doi: 10.1016/j.materresbull.2018.12.020.

[7] N. M. Mahmoodi, S. Keshavarzi, M. Oveisi, S. Rahimi, and B. Hayati, "Metal-organic framework (ZIF-8)/inorganic nanofiber (Fe_2O_3) nanocomposite: Green synthesis and photocatalytic degradation using LED irradiation," *Journal of Molecular Liquids,* vol. 291, p. 111333, 2019, doi: 10.1016/j.molliq.2019.111333.

[8] Y. Liu *et al.*, "Photostable core-shell CdS/ZIF-8 composite for enhanced photocatalytic reduction of CO_2," *Applied Surface Science,* vol. 498, p. 143899, 2019, doi: 10.1016/j.apsusc.2019.143899.

[9] J. Qiu *et al.*, "Constructing $Cd_{0.5}Zn_{0.5}S$@ZIF-8 nanocomposites through self-assembly strategy to enhance Cr(VI) photocatalytic reduction," *Journal of Hazardous Materials,* vol. 349, pp. 234-241, May 5 2018, doi: 10.1016/j.jhazmat.2018.02.009.

[10] X. Wei, Y. Wang, Y. Huang, and C. Fan, "Composite ZIF-8 with CQDs for boosting visible-light-driven photocatalytic removal of NO," *Journal of Alloys and Compounds,* vol. 802, pp. 467-476, 2019, doi: 10.1016/j.jallcom.2019.06.086.

[11] J. Liu *et al.*, "Photocatalytic conversion of nitrogen to ammonia with water on triphase interfaces of hydrophilic-hydrophobic composite $Bi_4O_5Br_2$/ZIF-8," *Chemical Engineering Journal,* vol. 371, pp. 796-803, 2019, doi: 10.1016/j.cej.2019.03.283.

[12] H.-T. Wang *et al.*, "Design and synthesis of porous C–ZnO/TiO_2@ZIF-8 multi-component nano-system via pyrolysis strategy with high adsorption capacity and visible light photocatalytic activity," *Microporous and Mesoporous Materials,* vol. 288, p. 109548, 2019, doi: 10.1016/j.micromeso.2019.06.010.

[13] Z. Li *et al.*, "Preparation of flexible PAN–C_3N_4–ZIF-8 photocatalytic nanofibers and visible light catalytic properties," *Optical Materials,* vol. 132, p. 112762, 2022, doi: 10.1016/j.optmat.2022.112762.

[14] T. Qiang, S. Wang, L. Ren, and X. Gao, "Novel 3D Cu_2O/N-CQD/ZIF-8 composite photocatalyst with Z-scheme heterojunction for the efficient photocatalytic reduction of Cr(VI)," *Journal of Environmental Chemical Engineering,* vol. 10, no. 6, p. 108784, 2022, doi: 10.1016/j.jece.2022.108784.

[15] D. Sajwan, A. Semwal, J. Rawat, H. Sharma, and C. Dwivedi, "Synthesis of CdSe QDs decorated ZIF-8 composite for visible light assisted degradation of methylene blue," *Materials Today: Proceedings,* 2022, doi: 10.1016/j.matpr.2022.10.008.

[16] J. Wu, Y. Jin, D. Wu, X. Yan, N. Ma, and W. Dai, "Well-construction of Zn_2SnO_4/SnO_2@ZIF-8 core–shell hetero-structure with efficient photocatalytic activity towards tetracycline under restricted space," *Chinese Journal of Chemical Engineering,* vol. 52, pp. 45-55, 2022, doi: 10.1016/j.cjche.2022.04.016.

[17] H. A. Yurtsever, M. Y. Akgunlu, T. Kurt, A. S. Yurttaş, and B. Topuz, "Photocatalytic activities of Ag^+ doped ZIF-8 and ZIF-L crystals," *Journal of the Turkish Chemical Society, Section A: Chemistry,* vol. 3, no. 3, 2016, doi: 10.18596/jotcsa.10970.

[18] G. Fan, J. Luo, L. Guo, R. Lin, X. Zheng, and S. A. Snyder, "Doping Ag/AgCl in zeolitic imidazolate framework-8 (ZIF-8) to enhance the performance of photodegradation of methylene blue," *Chemosphere,* vol. 209, pp. 44-52, Oct 2018, doi: 10.1016/j.chemosphere.2018.06.036.

[19] H. A. Yurtsever and A. E. Çetin, "Fabrication of ZIF-8 decorated copper doped TiO_2 nanocomposite at low ZIF-8 loading for solar energy applications," *Colloids and Surfaces A: Physicochemical and Engineering Aspects,* vol. 625, p. 126980, 2021, doi: 10.1016/j.colsurfa.2021.126980.

[20] N. Madkhali *et al.*, "Recent update on photocatalytic degradation of pollutants in waste water using TiO_2-based heterostructured materials," *Results in Engineering,* vol. 17, p. 100920, 2023, doi: 10.1016/j.rineng.2023.100920.

[21] R. Chandra, S. Mukhopadhyay, and M. Nath, "TiO_2@ZIF-8: A novel approach of modifying micro-environment for enhanced photo-catalytic dye degradation and high usability of TiO_2 nanoparticles," *Materials Letters,* vol. 164, pp. 571-574, 2016, doi: 10.1016/j.matlet.2015.11.018.

[22] E. Pipelzadeh, V. Rudolph, G. Hanson, C. Noble, and L. Wang, "Photoreduction of CO_2 on ZIF-8/TiO_2 nanocomposites in a gaseous photoreactor under pressure swing," *Applied Catalysis B: Environmental,* vol. 218, pp. 672-678, 2017, doi: 10.1016/j.apcatb.2017.06.054.

[23] R. Li, W. Li, C. Jin, Q. He, and Y. Wang, "Fabrication of ZIF-8@TiO_2 micron composite via hydrothermal method with enhanced absorption and photocatalytic activities in tetracycline degradation," *Journal of Alloys and Compounds,* vol. 825, p. 154008, 2020, doi: 10.1016/j.jallcom.2020.154008.

[24] X. Qi, F. Shang, T. Wang, Y. Ma, and Y. Yan, "In situ coupling of TiO_2(B) and ZIF-8 with enhanced photocatalytic activity via effective defect," *CrystEngComm,* vol. 22, no. 25, pp. 4250-4259, 2020, doi: 10.1039/d0ce00595a.

[25] W.-L. Zhong, C. Li, X.-M. Liu, X.-K. Bai, G.-S. Zhang, and C.-X. Lei, "Liquid phase deposition of flower-like TiO_2 microspheres decorated by ZIF-8 nanoparticles with enhanced photocatalytic

activity," *Microporous and Mesoporous Materials,* vol. 306, p. 110401, 2020, doi: 10.1016/j.micromeso.2020.110401.

[26] C. Hou, Q. Xu, J. Peng, Z. Ji, and X. Hu, "(110)-oriented ZIF-8 thin films on ITO with controllable thickness," *Chemphyschem,* vol. 14, no. 1, pp. 140-144, Jan 14 2013, doi: 10.1002/cphc.201200677.

[27] G. Genesio, J. Maynadié, M. Carboni, and D. Meyer, "Recent status on MOF thin films on transparent conductive oxides substrates (ITO or FTO)," *New Journal of Chemistry,* vol. 42, no. 4, pp. 2351-2363, 2018, doi: 10.1039/c7nj03171h.

[28] K. Kida, K. Fujita, T. Shimada, S. Tanaka, and Y. Miyake, "Layer-by-layer aqueous rapid synthesis of ZIF-8 films on a reactive surface," *Dalton Transactions,* vol. 42, no. 31, pp. 11128-11135, Aug 21 2013, doi: 10.1039/c3dt51135a.

[29] O. Shekhah and M. Eddaoudi, "The liquid phase epitaxy method for the construction of oriented ZIF-8 thin films with controlled growth on functionalized surfaces," *Chemical Communications,* vol. 49, no. 86, pp. 10079-10081, Oct 3 2013, doi: 10.1039/c3cc45343j.

[30] J. A. Allegretto, J. Dostalek, M. Rafti, B. Menges, O. Azzaroni, and W. Knoll, "Shedding Light on the Dark Corners of Metal-Organic Framework Thin Films: Growth and Structural Stability of ZIF-8 Layers Probed by Optical Waveguide Spectroscopy," *The Journal of Physical Chemistry A,* vol. 123, no. 5, pp. 1100-1109, Feb 7 2019, doi: 10.1021/acs.jpca.8b09610.

[31] R. L. Papporello, E. E. Miró, and J. M. Zamaro, "Secondary growth of ZIF-8 films onto copper-based foils. Insight into surface interactions," *Microporous and Mesoporous Materials,* vol. 211, pp. 64-72, 2015, doi: 10.1016/j.micromeso.2015.02.049.

[32] O. L. Rose *et al.*, "Thin Films of Metal-Organic Framework Interfaces Obtained by Laser Evaporation," *Nanomaterials,* vol. 11, no. 6, May 21 2021, doi: 10.3390/nano11061367.